



Matching a transducer to water at cavitation: Acoustic horn design principles

Sergei L. Peshkovsky, Alexey S. Peshkovsky *

Industrial Sonomechanics, LLC, 1505 St. Nicholas Avenue #5B, New York, NY 10033, USA

Received 14 February 2006; received in revised form 6 June 2006; accepted 1 July 2006

Available online 14 August 2006

Abstract

High-power ultrasound for several decades has been an integral part of many industrial processes conducted in aqueous solutions. Maximizing the transfer efficiency of the acoustic energy between electromechanical transducers and water at cavitation is crucial when designing industrial ultrasonic reactors with large active volumes. This can be achieved by matching the acoustic impedances of transducers to water at cavitation using appropriately designed ultrasonic horns. In the present work, a set of criteria characterizing the matching capabilities of ultrasonic horns is developed. It is shown that none of the commonly used tapered-shape horns can achieve the necessary conditions. An analytical method for designing five-element acoustic horns with the desirable matching properties is introduced, and five novel types of such horns, most suitable for practical applications, are proposed. An evaluation of the horns' performance is presented in a set of experiments, demonstrating the validity of the developed theoretical methodology. Power transfer efficiency increase by almost an order of magnitude is shown to be possible with the presented horn designs, as compared to those traditionally utilized.

© 2006 Elsevier B.V. All rights reserved.

Keywords: Ultrasonic rod horns; Electromechanical transducers; Acoustic impedance matching; Ultrasonic power transference; Acoustic energy transference; Acoustic horns; Industrial ultrasonic reactors; Sonochemistry; Industrial processes in liquids; Cavitation

1. Introduction

High-power ultrasound for several decades has been an integral part of many industrial processes conducted in weak aqueous solutions, such as cleaning, extraction, homogenizing, emulsification, sonochemistry, pollutant destruction, etc. [1–3]. These ultrasound-aided (macrosonics) processes are based on the effect of acoustic cavitation induced in water during intensive ultrasonic treatment. The electromechanical transducers used to convert the high frequency electric power into the ultrasonic power cannot, however, directly provide the necessary amplitudes of longitudinal ultrasonic vibrations to induce cavitation. Acoustic rod horns connected to the transducers are, therefore, used to amplify the vibration amplitude. Commonly used

acoustic horns have tapered shapes, such as conical, exponential, catenoidal, stepped, or more complex, and converge in the direction of the loads [3–5]. Although widely used, these horns suffer from an important limitation: they are incapable of providing matching between the transducers and the liquid loads, leading to an inefficient acoustic power transmission.

It is well known that for an optimal operation of an ultrasonic horn system, the maximum cross-sectional dimension of any portion of the resonant horn or transducer cannot exceed, approximately, a quarter-wavelength of the corresponding longitudinal acoustic wave at the horn's resonance frequency [6]. Consequently, a convergent horn with a maximal allowed base-width always ends up having a working tip dimension that is smaller than this limitation. The final size of the tip depends on the gain factor of the horn, and becomes reduced as the gain factor increases. This is problematic when the abovementioned

* Corresponding author.

E-mail address: alexey@sonomechanics.com (A.S. Peshkovsky).

processes are carried out on an industrial scale, since a deposition of substantial acoustic power is needed to create acoustic cavitation in large volumes of liquid. While using the converging horns permits increasing the specific acoustic power (or vibration amplitude) radiated by the electromechanical transducer into the load quite effectively, it is impossible to achieve the technologically necessary levels of total radiated acoustic power, since the cross-sectional area of the horn tip in contact with the load is small. Therefore, it is intuitive that the use of the convergent horns does not permit transferring all available power of an acoustic transducer into a load.

In actual practice a technique that is frequently attempted to circumvent this limitation is the use of a convergent horn with an extension in the form of a small disk at the end. This horn, however, usually works inadequately because when a disk of arbitrary dimensions is connected to a horn, the resonance frequency and the vibration amplitude conditions change dramatically, in comparison with the calculated values, and the horn's behavior becomes difficult to predict. Complicated experimental fitting of the parameters is then required for each horn. Additionally, the fatigue strength of the disk joint is low, which diminishes the horn's reliability and lifetime of operation. Rod horns connected to planar resonant systems, such as large discs or planes are also sometimes used [7]. Another solution attempted in the past was to develop an alternative reactor design with an incorporated converging horn [3].

In this manuscript we introduce novel design principles used for the development of a completely novel family of acoustic horns, whose shapes permit achieving high gain factors and large output surfaces simultaneously. These horns can be designed to accurately match an ultrasonic source to a liquid load at cavitation, maximizing the transference of the available acoustic energy into the load and creating a large cavitation volume. The devices are easy to machine and have well-isolated axial resonances and uniform output amplitudes, as shown in the experimental section.

2. Criteria for matching a magnetostrictive transducer to water at cavitation

Under the most convenient approximation, which is, nevertheless, quite suitable for the engineering calculations, the highest specific acoustic power that a well (perfectly) cooled resonant magnetostrictive transducer can transmit into a load is limited by two main factors – the magnetostrictive stress saturation, τ_m (the maximal mechanical stress achievable due to the magnetostrictive effect for a given transducer material), and the maximum allowed oscillatory velocity, limited by the fatigue strength of the transducer material, V_m , such that [8]

$$\begin{aligned} \tau_m &= e_m E \phi_1 \\ V_m &= \sigma_m \phi_2 / \rho c \end{aligned} \quad (1)$$

where e_m is the deformation amplitude associated with τ_m , E is Young's modulus, ϕ_1 and ϕ_2 are the coefficients that

take into account the features of the transducer construction [4,8], σ_m is the stress amplitude of the material fatigue strength, ρ is the transducer material's density, and c is the thin-wire speed of sound in the material. The highest specific power radiated under conditions of perfect matching between the transducer and the load is represented by the quantity

$$W_m = 0.5\tau_m V_m \quad (2)$$

Let us now consider the criteria, upon which an ultrasonic horn should be designed in order to achieve a matching condition between a transducer and a given load. As an acoustic load of the transducer, water at cavitation will be further considered as the most common and experimentally studied load encountered in technological applications of ultrasound. It should be noted that the acoustic load under consideration, water at cavitation, has a purely active character [9], and, therefore, is appropriately described by the term "acoustic resistivity", r_w . Practically, this means that virtually all of the acoustic energy deposited into water at cavitation is converted into heat [10]. Under the term "matching" we will further mean supplying an electromechanical transducer with a multi-element ultrasonic horn possessing a gain factor, $G \gg 1$ (G is defined as a ratio of the output to input oscillatory velocities, V/V_m), which allows the transference of a maximum of the available acoustic power of the transducer, W_m , into the load.

Specific acoustic power, W_1 , generated in a purely active load by the longitudinal vibrations of an acoustic rod horn with an output oscillatory velocity, V , is represented by

$$W_1 = 0.5r_w V^2 \quad (3)$$

Taking $W_m = W_1$ as a matching condition, we obtain

$$\frac{\tau_m}{r_w V} = GN^2 \quad (4)$$

where $N^2 = S_{out}/S_{in}$, S_{in} and S_{out} are, respectively, the input and the output cross-sections of the acoustic horn, while S_{in} is taken to be equal to the output cross-section of the electromechanical transducer, S_t (please see Fig. 1). The left-hand side of Eq. (4) reflects the degree of underloading of an acoustic transducer, and the right-hand side describes matching capabilities of an acoustic horn.

For a resonant system matched to an acoustic load, the traveling-wave factor can be presented as the ratio of the

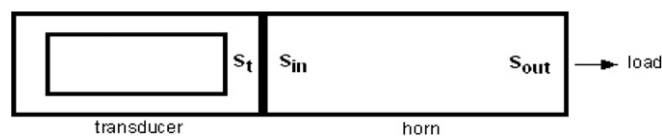


Fig. 1. General schematic is shown, describing matching between an electromechanical transducer and a load achieved by using an acoustic rod horn of an arbitrary shape. S_{in} and S_{out} are, respectively, the input and the output cross-sections of the acoustic horn; S_t is the output cross-section of the electromechanical transducer.

maximum energy radiated into the load to the maximum energy stored in the transducer in the form of a standing acoustic wave

$$k_t = \frac{\tau_m V_m}{\rho c V_m^2} = \frac{\tau_m}{\sigma_m \phi_2} \quad (5)$$

For the common magnetostrictive materials, τ_m is much smaller than σ_m , and, therefore, $k_t \ll 1$. This means that a standing-wave mode in the transducer matched to the load is always present. In addition, since the considered acoustic load has an active character, the resonance dimensions of the transducer and the horn are preserved.

From experimental studies [9] it is known that during the radiation of ultrasound into water at cavitation, the relationship $r_w V = \sqrt{2P_0}$, where P_0 is the hydrostatic pressure of water, remains, roughly, constant. Therefore, the following can be written:

$$\frac{\tau_m}{r_w V} = \frac{e_m E \phi_1}{\sqrt{2P_0}} \quad (6)$$

It is seen from Eq. (6) that the degree of the under-loading of an acoustic transducer depends only on the characteristics of the transducer itself and the hydrostatic pressure of water. For most common magnetostrictive materials, the calculated values of $\tau_m/r_w V$ are between 15 and 44. In this calculation, the values of $P_0 = 10^5 \text{ N/m}^2$ and $\phi_1 = 0.45$ were assumed.

Industrial acoustic transducers, generally, have their nominal electrical power W_e , efficiency factor η and output oscillatory velocity V_n , specified. The practical degree of the under-loading for such industrial magnetostrictive transducers can be, therefore, characterized by the relationship $2\eta W_e/r_w V V_n S_t$, having assumed that $W_m = \eta W_e/S_t$. The practical values of the degree of under-loading obtained from this expression are much lower than the corresponding theoretical limits for the magnetostrictive materials themselves, and for most models fall in the range between 3 and 5.

It is important to point out that in the case of piezoelectric transducers the highest achievable level of specific acoustic power is practically restricted by the electrical resilience of the entire apparatus, rather than by the properties of the piezoelectric material itself. The limiting value of maximal electric power is, generally, available from the transducer supplier and can also be used in this expression for the evaluation of the practical degree of under-loading of the industrial piezoelectric transducers.

It is less evident how to use the right-hand side of Eq. (4), which reflects the matching capabilities of a horn. The point to emphasize is that in spite of a variety of types and shapes of the acoustic horns known from the literature and used in practice, none exist, for which the relationship $GN^2 > 1$, when $G > 1$, would hold true. It is, therefore, clear that in order to be able to match ultrasonic transducers to water at cavitation, it is necessary to develop new

types of acoustic horns that would meet the matching criterion, $GN^2 > 1$.

3. Five-element matching horns

3.1. Design principles

The theory of acoustic horns is based on the problem of longitudinal vibrations of multi-element rods that have cylindrical elements and elements of variable cross-sections [11]. We will consider only the horns of axially symmetric shapes. Other types of horns (for example, wedge-shaped) can be considered in an analogous way. In the current work we will restrict the discussion to the five-element horns, although no theoretical restriction for the number of elements exists.

We assume that during the passage of the stress waves through a horn, the wave front remains planar, while the stresses are uniformly distributed over the horn's cross-section. This assumption limits us to the thin horns, whose resonance lengths significantly exceed their diameters. For all practical purposes, it is sufficient to require that the maximum cross-sectional dimension of any portion of a resonant horn not exceed, approximately, a quarter-wavelength of the corresponding thin wire acoustic wave at the horn's resonance frequency [6].

The schematic and the designation of parameters for a general case of a five-element rod horn are given in Fig. 2, where two possible situations are presented: a horn with $d_1/d_3 > 1$ is shown by the solid line; a horn with $d_1/d_3 < 1$ is shown by the dotted line. Under the assumed approximation, the problem is reduced to one-dimension, and it is limited to the consideration of elements with variable cross-section of only conical shape. For a steady-state mode, the equation of vibrations for displacements, u , takes the following form:

$$u'' + \frac{1}{S} S' u' + k^2 u = 0 \quad (7)$$

where $k = \omega/c$ is the wave number, $\omega = 2\pi f$ is the angular frequency of vibrations, and f is the frequency of vibrations.

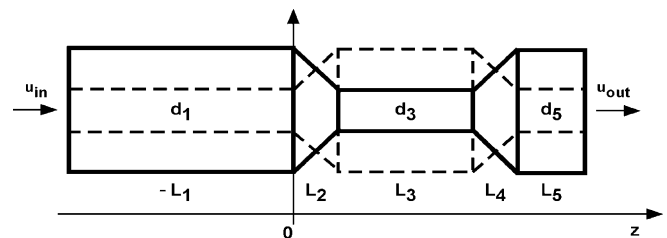


Fig. 2. Schematic defining the parameters of a five-element matching horn is shown. The horn having $d_1/d_3 > 1$ is shown by a solid line, and the horn with $d_1/d_3 < 1$ is shown by a dotted line. Parameters L_1 – L_5 correspond to the lengths of each element.

The solutions of Eq. (7) for each of the horn's elements can be written as

$$\begin{aligned}
 u_1 &= A_1 \cos kz + B_1 \sin kz; \quad -L_1 < z < 0 \\
 u_2 &= F(A_2 \cos kz + B_2 \sin kz); \quad 0 < z < L_2 \\
 u_3 &= A_3 \cos kz + B_3 \sin kz; \quad L_2 < z < L_2 + L_3 \\
 u_4 &= F(A_4 \cos kz + B_4 \sin kz); \quad L_2 + L_3 < z < L_2 + L_3 + L_4 \\
 u_5 &= A_5 \cos kz + B_5 \sin kz; \quad L_2 + L_3 + L_4 < z < L_2 + L_3 + L_4 + L_5
 \end{aligned} \quad (8)$$

Then, using the boundary conditions for the horn's element, we obtain the system of equations for displacements, u , and strains, u' .

$$\begin{aligned}
 \text{At } z = -L_1, \quad u_1 &= u_{\text{in}}, \quad ES_1 u'_1 = -F_{\text{in}}, \quad F_{\text{in}} = 0 \\
 A_1 \cos kL_1 - B_1 \sin kL_1 &= u_{\text{in}}; \\
 EkS_1(A_1 \sin kL_1 + B_1 \cos kL_1) &= -F_{\text{in}} \\
 \text{At } z = 0, \quad u_2 &= u_1, \quad u'_2 = u'_1 \\
 FA_2 = A_1; \quad F'A_2 + FB_2k &= kB_1; \\
 \alpha = (d_1 - d_3)/L_2d_1; \\
 F = 2/d_1; \quad F' = F\alpha \\
 \text{At } z = L_2, \quad u_3 &= u_2, \quad u'_3 = u'_2 \\
 A_3 \cos kL_2 + B_3 \sin kL_2 &= F(A_2 \cos kL_2 + B_2 \sin kL_2); \\
 -kA_3 \sin kL_2 + kB_3 \cos kL_2 &= (F'B_2 - FkA_2) \sin kL_2 + (F'A_2 + FkB_2) \cos kL_2; \\
 \alpha = (d_1 - d_3)/L_2d_1; \\
 F = 2/d_3; \quad F' = -F/(L_2 - 1/\alpha) \\
 \text{At } z = L_2 + L_3, \quad u_4 &= u_3, \quad u'_4 = u'_3 \\
 F[A_4 \cos k(L_2 + L_3) + B_4 \sin k(L_2 + L_3)] &= A_3 \cos k(L_2 + L_3) + B_3 \sin k(L_2 + L_3); \\
 (F'B_4 - FkA_4) \sin k(L_2 + L_3) + (F'A_4 + FkB_4) \cos k(L_2 + L_3) &= -kA_3 \sin k(L_2 + L_3) + kB_3 \cos k(L_2 + L_3); \\
 \alpha = (d_3 - d_5)/L_4d_3; \quad F = 2/d_3; \quad F' = F\alpha \\
 \text{At } z = L_2 + L_3 + L_4, \quad u_5 &= u_4, \quad u'_5 = u'_4 \\
 A_5 \cos k(L_2 + L_3 + L_4) + B_5 \sin k(L_2 + L_3 + L_4) &= F[A_4 \cos k(L_2 + L_3 + L_4) + B_4 \sin k(L_2 + L_3 + L_4)]; \\
 -kA_5 \sin k(L_2 + L_3 + L_4) + kB_5 \cos k(L_2 + L_3 + L_4) &= (F'B_4 - FkA_4) \sin k(L_2 + L_3 + L_4) \\
 &\quad + (F'A_4 + FkB_4) \cos k(L_2 + L_3 + L_4); \\
 \alpha = (d_3 - d_5)/L_4d_3; \quad F = 2/d_5; \quad F' = -F/(L_4 - 1/\alpha) \\
 \text{At } z = L_2 + L_3 + L_4 + L_5, \quad u_5 &= u_{\text{out}}, \quad u'_5 = 0 \\
 A_5 \cos k(L_2 + L_3 + L_4 + L_5) + B_5 \sin k(L_2 + L_3 + L_4 + L_5) &= u_{\text{out}}; \\
 -A_5 \sin k(L_2 + L_3 + L_4 + L_5) + B_5 \cos k(L_2 + L_3 + L_4 + L_5) &= 0
 \end{aligned} \quad (9)$$

The gain factor of the horn can be expressed as

$$\begin{aligned}
 G &= \left| \frac{u_{\text{out}}}{u_{\text{in}}} \right| \\
 &= \left| \frac{A_5 \cos k(L_2 + L_3 + L_4 + L_5) + B_5 \sin k(L_2 + L_3 + L_4 + L_5)}{A_1 \cos kL_1 - B_1 \sin kL_1} \right|
 \end{aligned} \quad (10)$$

where $F = 2/d_n$, d_n is the diameter of the corresponding cylindrical element of the horn, A_n and B_n are the constant coefficients for the corresponding elements of the horn, L_n is the length of the corresponding element of the horn, n is the order number of the horn element, α is the cone index of the horn element with variable cross-section, u_{in} and u_{out} are the amplitudes of displacements at the horn input and output, respectively. The boundary conditions for the force acting on the horn's input, $F_{\text{in}} = 0$, and for the strain at the horn output, $u'_5 = 0$, in this system of equations indicate that the horn has a total resonance length and does not have an acoustic load.

From the system of equation (9), one can obtain all necessary characteristics of a five-element horn: lengths and diameters of the elements, gain factor, distribution of vibration amplitudes, and distribution strains along the horn. From this system of equations, it is also easy to obtain solutions for any horns with conical elements (for example, with a number elements smaller than five). Horns with other shapes of the variable cross-section elements (for example, with exponential or catenoidal elements) can be considered in an analogous way, taking into account the variation of sound velocity in such elements.

3.2. Analysis of five-element horns

To solve the system of Eq. (9) and to present results in a convenient graphical form, a computer program has been written that allows all the indicated above characteristics of five-element horns to be obtained in real time for subsequent analysis. The input parameters are: operating frequency of the horn, acoustic properties and fatigue strength of the horn material, and the diameter-to-length ratios of the horn elements.

Out of all variety of possible types of five-element horns, let us consider the five horns that are most suitable for practical applications. For the convenience of a comparison of horn parameters, we further assume $N = d_1/d_5 = 1$. Fig. 3 shows a conical-cylindrical matching horn and its design parameters. This is the simplest degenerate horn with $L_1 = 0$. Such a horn has low matching capabilities, the maximum value being $GN^2 \approx 3$.

Fig. 4 shows a step matching horn and its design parameters. The maximum value of the matching capability of this horn is $GN^2 \approx 4$. Both horns considered above can be used to match industrial acoustic transducers of low power for exciting relatively low amplitudes of ultrasonic vibrations in the load. Their small resonance dimensions convenient for construction should be particularly noted.

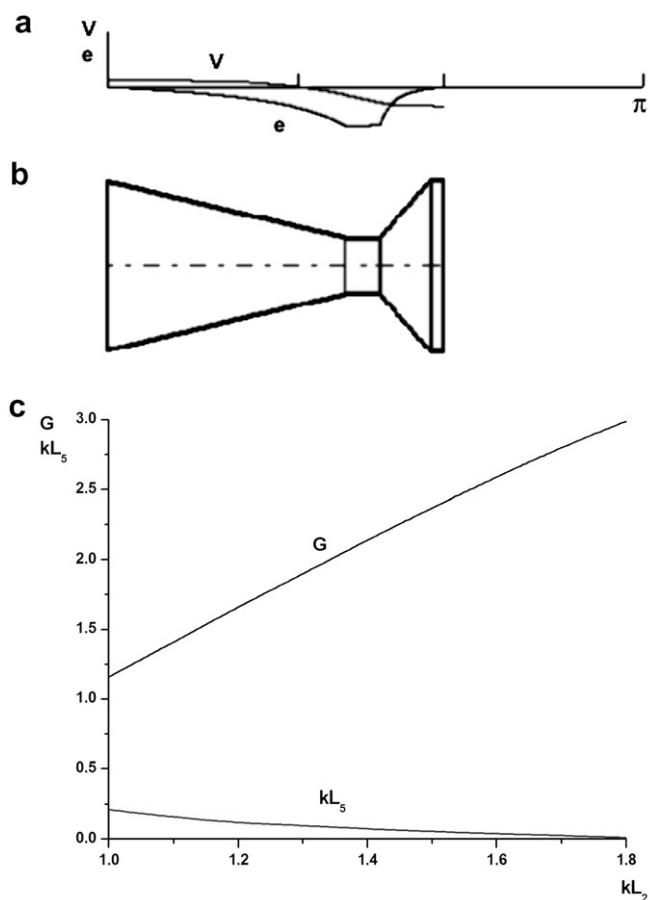


Fig. 3. Conical-cylindrical horn is shown with $d_1 = d_5$; $d_1/d_3 = 3.0$; $kL_1 = 0$; $kL_3 = 0.2$; $kL_4 = 0.3$, along with (a) the distribution of the oscillatory velocity, V , and strain, e , along the horn; (b) drawing of the horn; (c) plot of the distribution of the horn's parameters.

A barrel-shaped matching horn and its design parameters are shown in Fig. 5. This horn is quite promising for the matching of acoustic transducers of small cross dimensions or for the use as a booster. The maximum value of its matching capabilities at the given parameters is $GN^2 \approx 8$. It should be borne in mind that the diameter of the horn's heavy section, d_3 , under the considered approximation must not exceed about a quarter of the length of acoustic wave.

Fig. 6 shows a spool-shaped matching horn and its design parameters. This horn is atypical because its main radiating surface is lateral, and it mainly radiates a cylindrical wave into the load, as opposed to a plane wave radiated by other matching horns. Given a symmetric form of the horn, the gain factor is always equal to 1, the node of displacements is located in the middle, and lateral surfaces move in anti-phase. When using lateral radiation, the horn's matching capabilities are quite high since there are no limitations on the overall length. Such horn connected into a sequential string can radiate a cylindrical wave of high total power into the load and produce a well-developed cavitation region of a large volume.

Above, we have considered the horns whose lengths were less than or close to half the length of the acoustic wave in

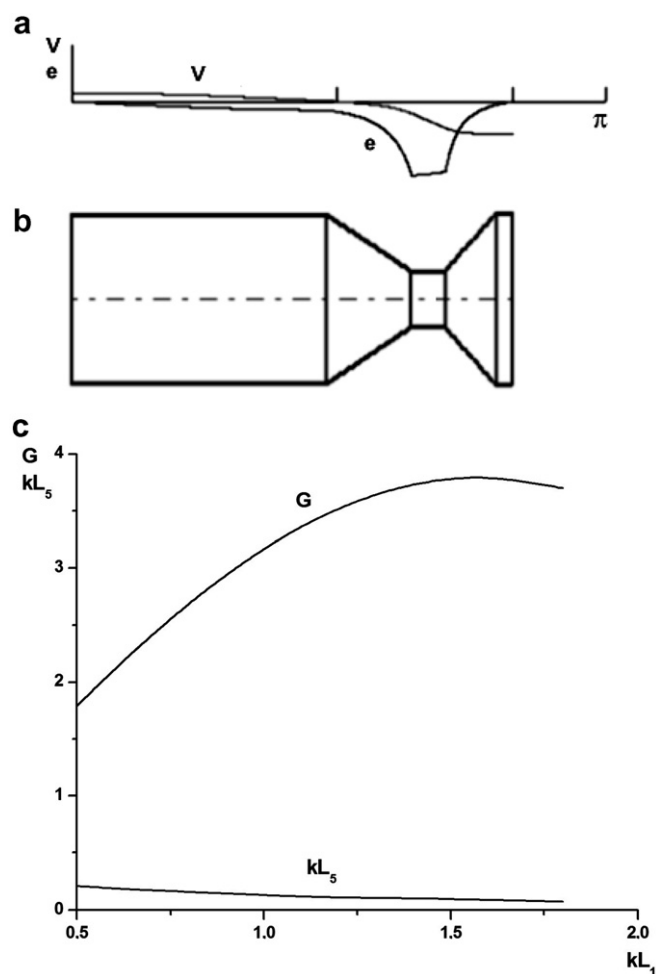


Fig. 4. Stepped horn is shown with $d_1 = d_5$; $d_1/d_3 = 3.0$; $kL_1 = 0.5$; $kL_3 = 0.2$; $kL_4 = 0.3$, along with (a) the distribution of the oscillatory velocity, V , and strain, e , along the horn; (b) drawing of the horn; (c) plot of the distribution of the horn's parameters.

the rod, the so-called half-wave horns. The system of Eq. (9) also allows one to obtain solutions for full-wave horns. One of such horns intended for the radiation of a plane acoustic wave of a very high power into water is a barbell-shaped horn shown in Fig. 7. Its design parameters, as a function of d_1/d_3 , are presented in Fig. 7(c). The matching capabilities of the barbell-shaped horn can reach the values of $GN^2 = 20$ or more. Such horn is very promising for the matching of high-power acoustic transducers that have large cross dimensions. For example, the highest design power radiated into the water at cavitation by this horn, made of titanium alloy, taking into account the fatigue strength limitations and limitations on output diameter under normal hydrostatic pressure, is about 5 kW at a frequency of 20 kHz. This value of the power of the acoustic radiation is close to the theoretically attainable maximum under the given conditions for any metallic rod horn. An expression for the theoretically attainable maximum power of acoustic radiation deposited into water under cavitation at a given frequency and electrostatic pressure, $W = P_0 V_m S_m$, can be obtained based on expressions 2 and 3,

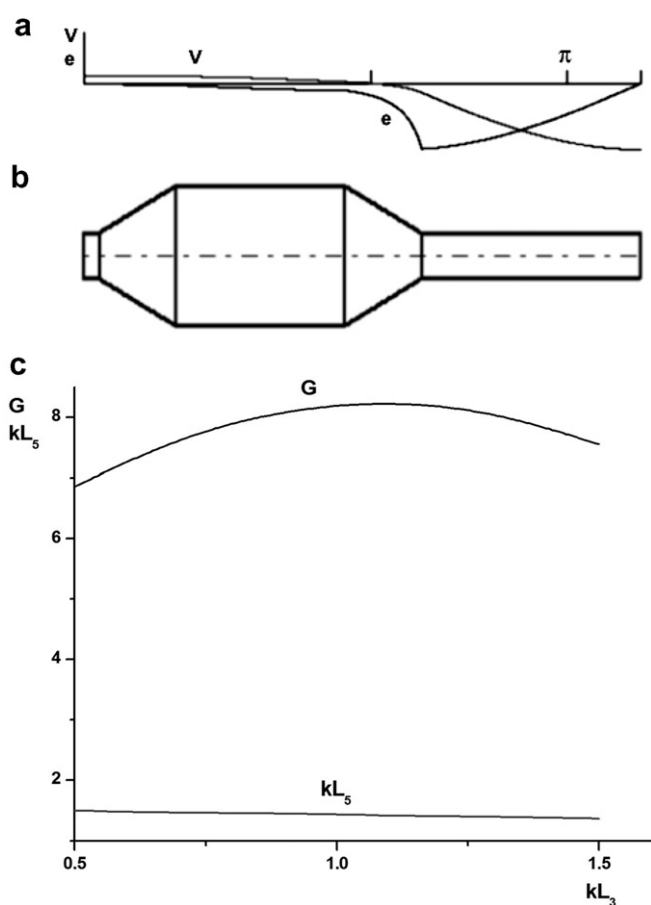


Fig. 5. Barrel horn is shown with $d_1 = d_5$; $d_3/d_1 = 3.0$; $kL_1 = 0.1$; $kL_2 = kL_4 = 0.5$, along with (a) the distribution of the oscillatory velocity, V , and strain, e , along the horn; (b) drawing of the horn; (c) plot of the distribution of the horn's parameters.

taking into account that $r_w V = \sqrt{2} P_0$. Here, S_m is the maximum possible area of the circular output surface of the acoustic horn, whose diameter is restricted by the quarter-wavelength condition mentioned above. The maximum achievable oscillation velocity, V_m , for best titanium alloys used as horn materials reaches, approximately, 10–15 m/s.

Due to the significant potential of the barbell-shaped horn for the industrial applications of ultrasound, we provide its exact parameters in Table 1. These parameters are convenient for the use during practical calculations.

3.3. Frequency characteristics of five-element horns

The knowledge of the frequency characteristics of an acoustic horn is very important when choosing the type of a matching horn for specific conditions of its excitation (type of an ultrasonic generator) and operation (properties of an acoustic load). These characteristics, according to (8), can be obtained by calculation in the form of a frequency dependence of the horn's input resistance. If losses are ignored, the expression for the input resistance of a five-element horn can be derived from the system of equation (9), assuming $z = F_{in}/j\omega u_{in}$. Taking $z_0 = EkS_{in}/\omega$, one can write

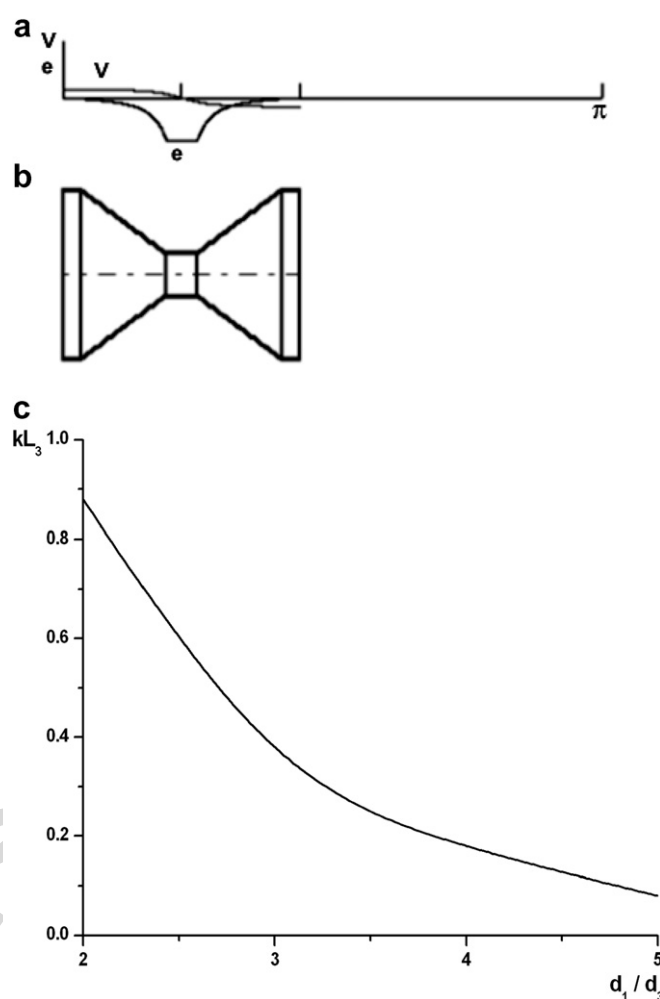


Fig. 6. Symmetrical spool-shaped horn is shown with $d_1 = d_5$; $kL_1 = kL_5 = 0.1$; $kL_3 = kL_4 = 0.5$, along with (a) the distribution of the oscillatory velocity, V , and strain, e , along the horn; (b) drawing of the horn; (c) plot of the distribution of the horn's parameters.

$$\frac{z}{z_0} = \frac{j(A_1 \sin kL_1 + B_1 \cos kL_1)}{A_1 \cos kL_1 - B_1 \sin kL_1} \quad (11)$$

The values of $|z/z_0|$ for the five-element horns considered above were calculated at a small change in the current frequency f , as compared with the horn natural frequency f_r , so that $(f_r - f)/f_r = 0.02$. Table 2 gives the values of $|z/z_0|$ obtained at the frequency, f , for the horns shown in Figs. 3–7 with similar gain factors, $G \approx 3$ (with the exception of the horn in Fig. 6). For comparison, the table also gives the values of $|z/z_0|$ for two resonant cylindrical rods that have characteristic lengths $kL = \pi$ and $kL = 2\pi$. It is evident that the presented values of $|z/z_0|$ characterize the rate of change in the horn's input resistance with a change in the frequency of excitation or the parameters of the acoustic load.

From Table 2 it is seen that the horn shown in Fig. 6 has the lowest frequency dependence of the input resistance. It is most suitable for the use in a sequentially connected string of such horns for the radiation of a cylindrical wave into the load. In this case, the low dependence of the horn input resistance on frequency is a positive property because when

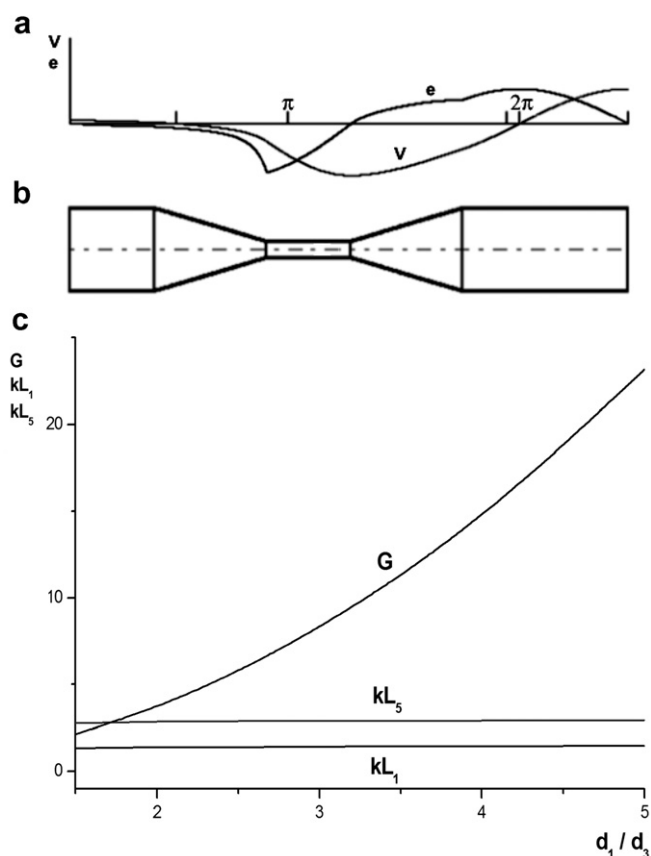


Fig. 7. Barbell-shaped horn is shown with $d_1 = d_5$; $kL_1 = kL_3$; $kL_2 = kL_4 = 0.5$, along with (a) the distribution of the oscillatory velocity, V , and strain, e , along the horn; (b) drawing of the horn; (c) plot of the distribution of the horn's parameters.

Table 1
Parameters convenient for practical calculations of barbell-shaped horns are provided

N	G	kL_1	kL_2	kL_5
1.5	2.176	1.383	0.405	2.853
2.0	3.527	1.290	0.693	2.725
2.5	4.918	1.245	0.916	2.640
3.0	6.285	1.224	1.099	2.574
3.5	7.597	1.216	1.253	2.519
4.0	8.834	1.215	1.386	2.470
4.5	9.987	1.217	1.504	2.426
5.0	11.049	1.222	1.609	2.384

Table 2
Values of $|z/z_0|$ obtained at the frequency, f , for the horns shown in Figs. 3–7 with similar gain factors, $G \approx 3$ (with the exception of the horn in Fig. 6), are provided. For comparison, the values of $|z/z_0|$ for two resonant cylindrical rods that have characteristic lengths, $kL = \pi$ and $kL = 2\pi$, are also given

Horn type	Cylinder $kL = \pi$	Cylinder $kL = 2\pi$	Fig. 3	Fig. 4	Fig. 5	Fig. 6	Fig. 7
$ z/z_0 $	0.063	0.126	0.09	0.14	0.345	0.024	0.67

several horns are connected in series, the analogous total dependence for the string will be also low. For horns with a gain factor greater than unity, the lowest dependence of

the input resistance on frequency is displayed by the horn shown in Fig. 3. The barbell-shaped full-wave horn is characterized by an abrupt dependence of input resistance on frequency. In this case, the positive feature is that a small error in dimensions during manufacturing of the horn has little influence on its resonance frequency. The horn can also reliably operate regardless of changes in its characteristic length, for example, if the reactive component of the acoustic impedance of the load changes. However, it should be noted that a barbell-shaped horn, due to the large diameter of its output surface, produces a plane wave in water at cavitation, during the radiation of which the reactive component of radiation impedance is virtually absent.

4. Experimental

For the experimental verification of the described horn design principles we have chosen the barbell-shaped horn, shown in Fig. 7. Direct calorimetric measurement of acoustic energy transmitted by this horn into water at cavitation was selected as a method of this horn's performance evaluation. The measurements of the acoustic energy absorbed in the cavitation region were conducted with the apparatus shown in Fig. 8. Settled tap water at a temperature of 20 °C

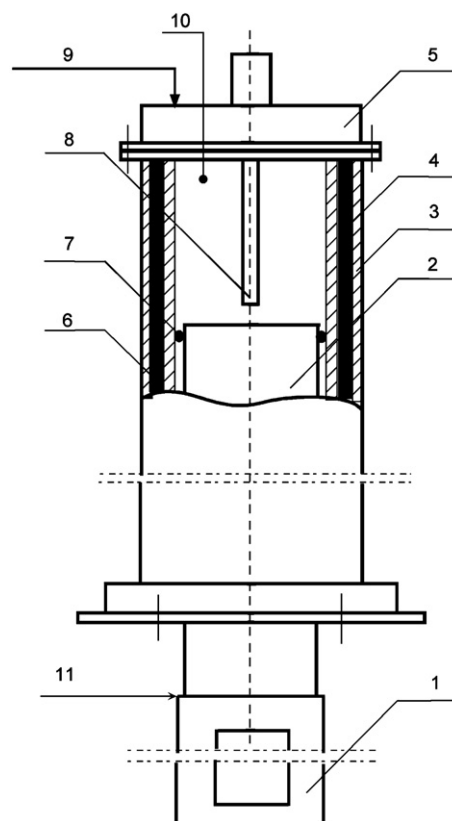


Fig. 8. Schematic of acoustic calorimeter is presented. 1 – magnetostrictive transducer, 2 – replaceable horn-radiator, 3 – external wall of calorimeter, 4 – heat insulation gasket, 5 – cover with porous sound-absorber, 6 – internal wall of calorimeter, 7 – sealing ring, 8 – set of thermocouples, 9 – gas supply, 10 – microphone, 11 – point of control over amplitude of transducer vibrations.

was used. The apparatus was based on an acoustic radiator consisting of a titanium horn connected to a magnetostrictive transducer, which operated at the resonance frequency of 17.8 kHz. The working power of the ultrasonic generator coupled to the magnetostrictive transducer was 5 kW. The oscillation amplitude of the magnetostrictive transducer was kept constant in all experiments at 1.67 m/s (rms). It was measured by placing a magnetic ring with an inductive coil on the transducer next to its output surface. Voltage was created in the coil as the transducer oscillated. The amplitude of this voltage corresponded to the oscillation amplitude and was measured by an oscilloscope. Prior calibration of this device was performed, in which the vibration amplitude was measured directly by a microscope.

A set of replaceable barbell-shaped horns was constructed to provide the necessary stepped change in the amplitude of the oscillatory velocity of the output end in contact with water. The set consisted of nine such horns with different gain factors (greater or smaller than unity), all of which had equal input and output diameters of 60 mm. Maximum oscillation velocity of some of these horns reached very large values, close to maximum theoretically possible for the best titanium alloys. Greatest achieved oscillation velocity was 12 m/s (rms). Therefore, maximum gain factor for the set was 7.2.

Static pressure in the calorimeter was produced with compressed nitrogen. The measurements of the resulting temperature of water were performed using a set of thermocouples. A change in the temperature of water during ultrasonic treatment was not more than 2–5 °C.

Fig. 9 shows an experimentally obtained plot of the specific acoustic power absorbed in the cavitation area, as a function of the oscillatory velocity of the horns' output radiating surfaces, at a static pressure of 1 bar. For the purpose of the measurement precision evaluation, data from Ref. [9] is also provided in the figure for the acoustic radi-

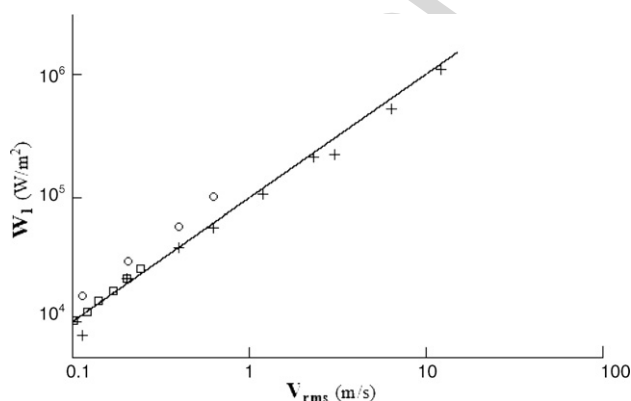


Fig. 9. Dependence of the intensity of the acoustic energy absorbed in the cavitation area is presented as a function of the oscillation velocity of the horns' output surfaces for a set of nine horns with different gain factors (+ are the data points from this work for the load pressure of 1 bar, ○ are the data points from this work for the load pressure of 2 bars, □ are the data points from Ref. [9]).

ation frequency of 19 kHz and the static pressure of 1 bar. The figure shows that the experimental data obtained in this work in the small oscillation velocity range corresponds very well to the data from Ref. [9]. Unfortunately, for large vibration velocities, no literature data was found. Performance verification of the horns with different gain factors conducted during the experiments showed that all of them possessed resonance and gain characteristics well corresponding to the theoretically predicted values. In no case was it necessary to make any adjustments to the horns after they were originally machined.

Fig. 9 additionally shows a curve corresponding to the Eq. (3), $W_1 = 0.5r_w V^2 = r_w V_{rms}^2 = P_0 V_{rms}$. The fact that the experimental data follows the curve very well shows that the relationship, $r_w V = \sqrt{2P_0}$, suggested in Ref. [9] and verified there for the small oscillation velocities, is maintained also for the significantly larger oscillation velocities. Thus, it has been experimentally proven that the matching between our barbell-shaped acoustic horns and water at cavitation truly takes place, in accordance with the theory presented above, for all possible oscillation velocities of the horns' output surfaces.

To demonstrate the effect of the elevated static pressure, Fig. 9 also shows the experimental data corresponding to the static pressure of 2 bars. It is clearly seen that increasing the pressure augments the absorbed acoustic energy in the cavitation area.

The region of the specific power with the values above 10^5 W/m² is very little studied, especially from the technological standpoint. The reason for this, from our perspective, is that the traditional cone-shaped horns, widely used in ultrasonic technology, are incapable of providing a large total radiation power, since their oscillation amplitudes are inversely proportional to the areas of their output surfaces. At large gain factors, the output surface area becomes very small, which complicates the development of sonochemical reactors capable of processing significant volumes of liquids. Thus, for example, a traditional stepped horn having an input diameter of 60 mm and a gain factor of 7.2 has the output diameter of, approximately, 20 mm. Therefore, at the maximum experimentally achieved specific power of 10^6 W/m², this stepped horn is capable of depositing not more than 300 W into its liquid load. Our barbell-shaped horn, used in the experiments presented in this section, on the other hand, delivers, approximately, 2.7 kW of total power, providing a power transfer efficiency increase by almost an order of magnitude.

A well-known method, described in detail in Ref. [12], was used for the experimental verification of the chemical activity in the cavitation area. The chemical activity level was determined by monitoring the oxidation reaction of KI in aqueous solution, resulting in the formation of free iodine. The obtained data is presented in Fig. 10. It can be clearly seen that the specific (divided by the horn's output surface area) rate of the concentration of the free iodine formation in the cavitation volume increases with the augmented intensity of the acoustic radiation. Total

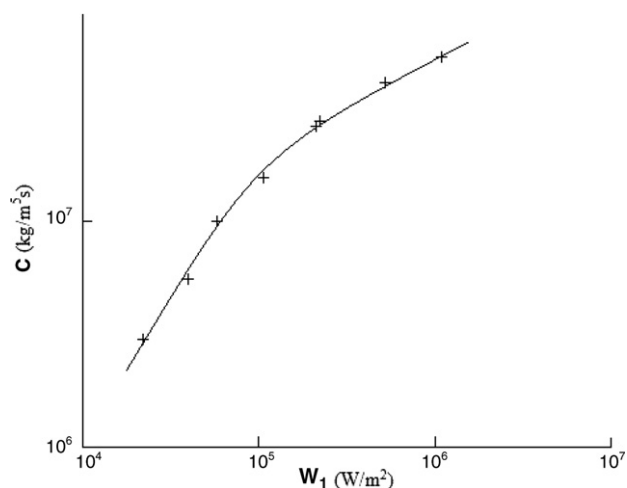


Fig. 10. Dependence of the specific (divided by the horn's output surface area) rate of the concentration of the free iodine formation in the cavitation volume is shown as a function of the intensity of the absorbed acoustic radiation.

increase of the concentration of the reduced iodine at maximum intensity of acoustic radiation of 10^6 W/m^2 reaches $1.5 \times 10^5 \text{ kg/m}^3 \text{ s}$.

5. Conclusions

Matching an ultrasonic transducer to a liquid load is a matter of choosing the matching horn that ensures the expression (4) at a given gain factor G , and of subsequent calculation of its resonance dimensions with the use of the system of Eq. (9). As stated above, when matching to an active acoustic load with $k_t \ll 1$, the standing acoustic wave in the transducer and in the horn is not disturbed, and their resonance dimensions do not change. The most powerful horn, from the designs described above, is the barbell-shaped horn, which was chosen for the experimental investigations. During the experiments, performance evaluation of a set of such horns with different gain factors showed that all of them had the resonance and the gain factor characteristics that corresponded very well to those predicted theoretically. It was also experimentally verified that matching of the acoustic horns with water at cavitation, according to the theory described above, is truly established for all possible values of the output oscillation velocities of the horns.

It should be noted that matching an acoustic transducer to a load using an acoustic horn is not the only possible method of matching. Another powerful matching factor, which results from the specific properties of water at cavitation, is hydrostatic pressure P_0 , according to the expression (6) and the experimental results presented here. It was also previously theoretically demonstrated that an increase in the load's hydrostatic pressure leads to an augmentation of the intensity of acoustic radiation [13], further resulting in an increase in the technological effectiveness of cavitation. It is evident that the best results are obtained when these two matching techniques are used jointly.

In conclusion, we would like to point out that our barbell-shaped horns also perform well in low-viscosity non-aqueous liquids and solutions, and permit building very effective sonochemical reactors for conducting experiments with these systems. This makes the described technology very attractive for the studies involving secondary effects of cavitation, such as sonoluminescence and sonofusion [14,15], which have been receiving a lot of attention recently.

References

- [1] A. Shoh, IEEE Trans. Sonics Ultrasonics su-22 (1975) 60.
- [2] T.J. Mason, Ultrason. Sonochem. 10 (2003) 175.
- [3] U.S. Bhirud, P.R. Gogate, A.M. Wilhelm, A.B. Pandit, Ultrason. Sonochem. 11 (2004) 143.
- [4] E. Eisner, in: W.P. Mason (Ed.), Methods and Devices, Part B, vol. 1, Academic Press, New York, 1964.
- [5] S. Sherrit, S.A. Askins, M. Gradziol, B.P. Dolgin, X.B.Z. Chang, Y. Bar-Cohen, in: Proceedings of the SPIE Smart Structures Conference, San Diego, CA 4701, Paper No. 34, 2002.
- [6] J.W. Rayleigh (Strutt), The Theory of Sound, New York, 1945.
- [7] A. Gallego-Juárez, G. Rodríguez-Corral, E. Riera-Franco de Sarabia, C. Campos-Pozuelo, F. Vázquez-Martínez, V.M. Acosta-Aparicio, Ultrasonics 38 (2000) 331.
- [8] Y. Kikuchi, in: Y. Kikuchi (Ed.), Ultrasonic Transducers, Corona Publ. Co., Tokyo, 1969.
- [9] K. Fukushima, J. Saneyoshi, Y. Kikuchi, Ultrasonic Transducers, in: Y. Kikuchi (Ed.), Corona Publ. Co., Tokyo, 1969.
- [10] E.F. Neppiras, Ultrasonics 3 (1965) 9.
- [11] L.G. Merkulov, A.B. Kharitinov, Sov. Phys. – Acoust. (1959) 183.
- [12] Sin Pin Lin, J. Acoust. Soc. Am. 36 (1964) 5.
- [13] L.D. Rosenberg (Ed.), High-intensity Ultrasonic Fields, Plenum Press, New York, 1971.
- [14] R.P. Taleyarkhan, C.D. West, J.S. Cho, R.T. Lahey Jr., R.I. Nigmatulin, R.C. Block, Science 295 (2002) 1868.
- [15] D.J. Flannigan, K.S. Suslick, Nature 434 (2005) 52.